Effects of Deletions at the Carboxyl Terminus of *Zymomonas mobilis* Pyruvate Decarboxylase on the Kinetic Properties and Substrate Specificity†

Alan K. Chang, Peter F. Nixon, and Ronald G. Duggleby*

Centre for Protein Structure, Function and Engineering, Department of Biochemistry, The University of Queensland, Brisbane QLD 4072 Australia

Received February 4, 2000; Revised Manuscript Received May 25, 2000

ABSTRACT: The three-dimensional structure of *Zymomonas mobilis* pyruvate decarboxylase shows that the carboxyl-terminal region of the protein occludes the active site. This observation is consistent with earlier suggestions that the active site is inaccessible to solvent during catalysis. However, the carboxyl-terminal region must move aside to allow entry of the substrate, and again to permit the products to leave. Here we have examined the role of the carboxyl terminus by making 15 variants of the enzyme with serial deletions. The activity is largely unaffected by removal of up to seven residues but deletion of the next two, R561 and S560, results in a drastic loss of activity. Five of these deletion mutants were purified and fully characterized and showed progressive decreases in activity, in the ability to discriminate between pyruvate and larger substrates, and in cofactor affinity. Several substitution mutants at residues R561 and S560 were prepared, purified, and fully characterized. The results indicate important roles for the side-chain of R561 and the backbone atoms of S560. It is suggested that the carboxyl-terminal region of pyruvate decarboxylase is needed to lock in the cofactors and for the proper closure of the active site that is required for discrimination between substrates and for decarboxylation to occur.

Pyruvate decarboxylase (PDC,[1] EC 4.1.1.1) is a member of a large family of enzymes that use thiamin diphosphate (ThDP) as a cofactor (*1*). The three-dimensional structures of several members of this family have now been determined, including PDC from yeast (*2*−*4*) and *Zymomonas mobilis* (*5*). In all cases, the active site of ThDP-dependent enzymes is at a domain interface and, with the exception of pyruvate:ferredoxin oxidoreductase (*6*), these domains are derived from different subunits. One domain contains the ThDP motif first identified by Hawkins et al. (*7*) and which binds a metal ion that in turn anchors ThDP to the enzyme via coordination to two of the phosphate oxygen atoms. The other domain contains the catalytic glutamate that is believed to promote the reactivity of the C2 atom of the thiazole ring (*8*).

Several workers have suggested that the active site of PDC is inaccessible to solvent-derived protons during catalysis (*9*−*11*). This notion of a closed active site agrees with earlier studies (*12*, *13*) in which it was proposed that a hydrophobic environment is required for the decarboxylation step in the reaction. Modeling (*14*) and kinetic (*15*, *16*) studies have further reinforced the idea of a cyclic opening and closing of the active site during catalysis. Active site closure would provide the right environment for catalysis to occur and might also prevent decomposition (*17*) of ThDP adducts that are intermediates in the PDC reaction.

On the basis of the first yeast PDC structure (*2*), Lobell and Crout (*14*) suggested that residues 106−113, 292−301, or the carboxyl terminus might participate in closure of the active site by acting as a "lid" since each of these regions is invisible in the structure and therefore presumed to be flexible. This was a reasonable proposal because the residues at the boundaries of these regions (e.g., 105 and 114) were not far from the position of ThDP in the structure. Candy and Duggleby (*1*) nominated residues 106−113 as the critical "lid" region but the determination of the structure of *Z. mobilis* PDC (*5*) suggests a more likely alternative.

This structure shows that the carboxyl-terminal region consists of an α-helix (E546−S560) connected to a tail (R561−K566) that together span the subunit interface (Figure 1A). ThDP is wedged in this interface but is inaccessible to solvent with only C2 of the ThDP thiazole ring, the atom that attacks the substrate, protruding from the underlying surface (Figure 1B). However, it should be noted that the position of C2 has been deduced from the locations of the remaining atoms of the thiazole ring; in the published structure, ThDP has undergone some degradation so that it is missing C2. For this reason, the enzyme cannot possibly be active. It is conceivable that these two features are connected and that the carboxyl-terminal region does not close over the active site when the true cofactor is present. However, as noted above, there are several lines of evidence that the active site is closed during catalysis and Dobritzsch et al. (*5*) proposed that the carboxyl-terminal region moves aside to allow substrate access and then closes during catalysis. Presumably, it then opens again to release the reaction products.

† This work supported by the Australian Research Council (Grant A09800834).

* To whom correspondence should be addressed. Phone: +617 3365 4615. Fax: +617 3365 4699. E-mail:duggleby@biosci.uq.edu.au.

[1] Abbreviations: bp, base pairs; PCR, polymerase chain reaction; PDC, pyruvate decarboxylase; SDS−PAGE, sodium dodecyl sulfate−polyacrylamide gel electrophoresis; ThDP, thiamin diphosphate.

10.1021/bi0002683 CCC: $19.00
Published on Web 07/11/2000

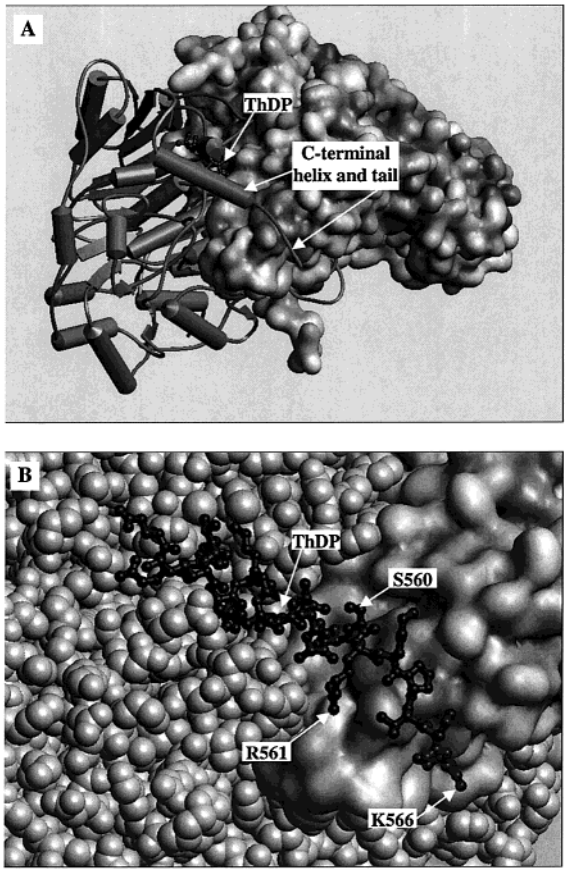

FIGURE 1: Structure of *Z. mobilis* PDC. In panel A, two of the four subunits are shown with one of the pair in schematic form and the other in a surface rendition. The carboxyl-terminal region of the former subunit comprising an α-helix (E546 to S560) and a tail (R561−K566) are indicated, together with ThDP which is partially eclipsed by the α-helix. The positions of the last two residues of the protein (L567 and L568) are not defined in the published structure. Panel B shows an expanded view of the carboxyl-terminal region with the α-helix and tail (residues E546 to K566) of the left subunit shown in ball-and-stick representation with the positions of S560, R561, and K566 indicated. The remainder of the left subunit is shown as CPK spheres. ThDP is buried in the underlying surface, apart from the deduced location of C2, which is shown by an arrow. Coordinates were determined by Dobritzsch et al. (*5*) and taken from the Protein Data Bank (1ZPD).

To investigate this hypothesis we have made a series of carboxyl-terminal deletions of the enzyme and find that the activity is largely unaffected by removal of seven residues but deletion of a further two (R561 and S560) results in a drastic loss of activity. The lowered activity is accompanied by a decreased affinity for the cofactors and a relaxation of substrate specificity so that the enzyme shows a reduced ability to discriminate between pyruvate, 2-ketobutyrate, and 2-ketovalerate. The nature of the residue at position 561, but not at 560, appears to be important as shown by mutated enzymes in which each of these residues was substituted.

EXPERIMENTAL PROCEDURES

Materials. Restriction enzymes, T4 DNA ligase, T4 DNA polymerase, and Klenow fragment were purchased from New England Biolabs (Beverly, MA). Exonuclease III and S1 nuclease were obtained from Promega (Sydney, Australia) and deoxyribonucleotides from Perkin-Elmer (Norwalk, CT). For sequencing we used the Prism Ready Dye Deoxy Terminator Cycle Sequencing Kit from Perkin-Elmer Applied Biosystems.

Bacterial culture, plasmid DNA preparations, restriction endonuclease digestions, ligations, and transformations were carried out according to standard protocols (*18*). *Escherichia coli* strain JM109 was obtained from Promega (Madison, WI). The pPLZM-PDC plasmid for heat-inducible PDC expression has been described previously (*19*). All *E. coli* cultures containing the wild-type and the mutant constructs were maintained on Luria broth plates with 100 μg/mL ampicillin. For long-term storage, liquid cultures were kept in 15% glycerol and stored at −70 °C.

Mutagenesis. Mutants with serial deletions at the carboxyl terminus were constructed using a protocol developed from Promega's Erase-a-Base System. pPLZM-PDC, which contains a *Xho*I site 22 bp downstream of the PDC gene stop codon, was cut with *Xho*I and the linearized DNA with 5′-overhangs was subjected to limited digestion with exonuclease III to generate a family of fragments that have 20−100 bases removed. The resulting collection of DNA fragments was treated with S1 nuclease to remove the 5′-overhangs and yield blunt-ended DNA fragments. These were then ligated in the presence of a double-stranded linker DNA with the palindromic sequence 5′-TGACTCGAGTCA-3′ to provide a stop codon (TGA). DNA sequencing of clones obtained in this way identified those that contained the stop codon in the correct reading frame, and these were used for PDC expression without further subcloning.

Variants with seven residues deleted and the next residue (R561) replaced by another amino acid were constructed using the complementary pair of primers shown below. *Sac*II, *Eco*RV, and *Sph*I recognition sites are underlined, the residue 561 codon is double-underlined, and lowercase letters 5′ to the 561 codon indicate a change from the wild-type sequence.

```
        SacII          561   EcoRV SphI
5′-GTTGCcGCgGCCAACAGCnnsTGAGATATCGCATGCACGC-3′
                             TATAGCGTACGTGCG-5′
```

The 5′-overhang was filled in using the Klenow fragment of *E. coli* DNA polymerase I. The resulting DNA was cut with *Sac*II and *Sph*I and then ligated to *Sac*II/*Sph*I-digested pPLZM-PDC. Positive clones were identified by the presence of the introduced *Eco*RV site in the primer. DNA sequencing identified the actual base changes at the degenerate positions.

The additional deletion mutants Δ7 and Δ9 were constructed by PCR, using the primers shown in Table 1. A DNA fragment, which comprises the second half of the PDC gene, was generated by PCR using the forward primer F/P1 with R/Δ7 or R/Δ9 as the reverse primer. The PCR product, which contains a single *Nco*I and *Xho*I site, was cut with these enzymes and used to replace the corresponding fragment of the wild-type gene in pPLZM-PDC. The mutants Δ8, Δ8+E, and Δ8+L were constructed in a similar way using the forward primer F/P2 and the reverse primer R/Δ8, R/Δ8+E, or R/Δ8+L, respectively.

Expression, Protein Purification, and Preparation of Apoenzyme. For expression of PDC on a 2 L scale, the cells were grown in 2YT medium (*18*) containing 100 μg/mL ampicillin at 30 °C. When the cell culture reached an A_{600} of 0.5 the temperature was increased rapidly to 42 °C and the induction was maintained for 3 h. The cells were harvested by centrifugation at 4 °C for 15 min at 2500*g* and

Table 1: Oligonucleotide Primers Used for PCR Mutagenesis[a]

Primer	Sequence
F/P1	5'-CCGCATTTGATGCTATCGG-3'
F/P2	5'-GACCGGCAAGCGCATTGTTCA-3'
R/Δ7	3'-GCGCAACGACGGCGGTTGTCGGCAACT*GAGCTC*GCC-5'
R/Δ8	3'-TTCGCGCAACGACGGCGGTTGTCGACT*GAGCTC*GCC-5'
R/Δ9	3'-CCATTCGCGCAACGACGGCGGTTGACT*GAGCTC*GCC-5'
R/Δ8+E	3'-CGACGGCGGTTGTCGcttACT*GAGCTC*CGGAGC-5'
R/Δ8+L	3'-CGACGGCGGTTGaAwACT*GAGCTC*CGGAGC-5'

[a] Reverse primers are shown 3′→5′ with the complement to the stop codon (TCA) double-underlined. Lowercase letters indicate a change from the wild-type sequence in the region preceding this stop codon. The restriction site for *Xho*I is in italics and underlined.

the cell pellet was stored at −20 °C. The purification of PDC was based on the protocol described previously (*20*). The purified enzyme was stored at −20 °C. Removal of cofactors to yield the apoenzyme was performed using our published procedure (*21*, *22*).

Activity Assay for PDC. PDC activity was measured in a coupled enzyme assay in which the rate of acetaldehyde production from 5 mM pyruvate was determined by following the oxidation of NADH at 340 nm and 30 °C in the presence of alcohol dehydrogenase (*21*). Reactions were started by addition of PDC using an amount of enzyme chosen so that a steady decrease of NADH concentration could be monitored over 5 min. In cell extracts and during enzyme purification, assays were performed with and without addition of alcohol dehydrogenase. The latter was taken as a measure of the lactate dehydrogenase activity that is present in cell extracts but is separated during purification (*22*). The K_m value for pyruvate was determined in the standard assay mixture with varying concentrations of substrate. This standard assay contains concentrations of ThDP (0.1 mM) and Mg^{2+} (5 mM) that are saturating for wild-type PDC. However, for all studies on the Δ15 mutant (including cofactor activation and binding), these concentrations were increased to 1 and 20 mM, respectively.

Measurement of Cofactor Activation and Cofactor Binding. Cofactor activation studies were carried out by measuring the activity of the reconstituted holoenzyme. The apoenzyme was preincubated for 15 min at 30 °C with NADH/alcohol dehydrogenase and a saturating concentration of one cofactor while varying the concentration of the other. The reaction was started by addition of 5 mM pyruvate and the data obtained were analyzed as described below.

Cofactor binding was measured by monitoring the quenching of tryptophan fluorescence of PDC (*21*) as a function of time using a Jasco model FB-770 spectrofluorimeter. Excitation was at 300 nm (band width 5 nm) and emission was measured at 340 nm (band width 5 nm).

Protein Analysis. SDS−PAGE was performed as described by Laemmli (*23*) and proteins were detected by staining with 0.1% (w/v) Coomassie blue. For routine measurements of protein concentrations, the dye-binding method of Sedmac and Grossberg (*24*) was used. Gel filtration chromatography was performed on a Pharmacia FPLC system using a Superdex 200 HR 10/30 column in 50 mM sodium phosphate buffer (pH 6.6) containing 0.15 M NaCl. The column was calibrated using as standards apoferritin (443 kDa), β-amylase (200 kDa), ADH (150 kDa), albumin (66 kDa), and carbonic anhydrase (29 kDa).

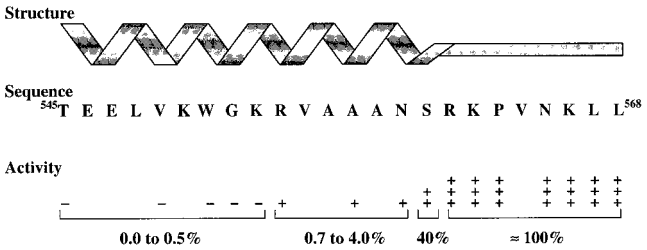

FIGURE 2: Carboxyl terminus of *Z. mobilis* PDC and the activity of serial deletion mutants. The structure is represented in cartoon form above the sequence from T545 to L568. The activity of deletion mutants, relative to that of wild-type, is then shown as high [(+++) ≈100%], moderate [(++) ≈40%], low [(+) 0.7−4.0%], and indetectable [(−) ≤0.5%]. If no symbol is shown, that mutant was not tested.

Data Analysis. Most experiments were repeated two or three times, and we observed good agreement between replicate experiments. The results reported represent the combined results from these replicates.

Kinetic parameters were determined by fitting the appropriate equation to the data by nonlinear regression using InPlot (GraphPad Software, San Diego, CA), GraFit (Erithacus Software, Staines, U.K.) or an adaptation of the DNRP53 program (*25*). The best fit values and standard errors obtained from these analyses are reported. Substrate and cofactor saturation curves were fitted to eq 1 to obtain values of V_m and K, where the latter represents the Michaelis constant (K_m) when X is a substrate, or the cofactor activation constant (K_c) values when X is a cofactor. Values of k_{cat} were calculated from V_m using the known concentration of enzyme (see below) that was present in the assay.

$$v = \frac{V_m[X]}{K + [X]} \quad (1)$$

Results of tryptophan fluorescence quenching experiments were analyzed according to Diefenbach and Duggleby (*21*). Briefly, the fluorescence values (F_t) as a function of time (t) were fitted using exponential decay curve (eq 2) from an initial fluorescence (F_o) to a final value (F_∞) to obtain an apparent first-order rate constant (k') at a given cofactor concentration.

$$F_t = (F_o - F_\infty)\exp(-k't) + F_\infty \quad (2)$$

The slope of the linear relationship (eq 3) between this rate constant and the cofactor concentration [C] represents the rate constant for association (k_{on}), while the rate constant for cofactor dissociation (k_{off}) is obtained from the intercept on the ordinate.

$$k' = k_{on}[C] + k_{off} \quad (3)$$

RESULTS

Serial Carboxyl-Terminal Deletions. Initially, a series of carboxyl-terminal deletion mutants were constructed, expressed, and assayed for PDC activity in cell extracts (Figure 2). Deletion of seven residues, up to and including K562,

Table 2: Kinetic Properties of Wild-Type and Deletion Mutants of PDC

enzyme	wild-type	Δ7	Δ8	Δ9	Δ11	Δ15
specific activity (units/mg)	95	103	24.3	4.5	3.4	0.12
pyruvate						
k_{cat} (s^{-1})	113 ± 1	135 ± 1	28.6 ± 0.1	5.29 ± 0.02	3.80 ± 0.02	0.18 ± 0.00
K_m (mM)	0.68 ± 0.02	1.35 ± 0.02	1.39 ± 0.02	0.82 ± 0.01	0.51 ± 0.01	0.50 ± 0.03
k_{cat}/K_m (mM^{-1} s^{-1})	166 ± 4	101 ± 1	20.5 ± 0.2	6.43 ± 0.08	7.40 ± 0.10	0.35 ± 0.01
2-ketobutyrate						not determined
k_{cat} (s^{-1})	61.4 ± 0.4	82.2 ± 0.4	30.1 ± 0.2	10.3 ± 0.11	26.0 ± 0.6	
K_m (mM)	2.86 ± 0.06	4.44 ± 0.07	8.86 ± 0.18	16.1 ± 0.4	15.3 ± 0.8	
k_{cat}/K_m (mM^{-1} s^{-1})	21.5 ± 0.4	18.5 ± 0.2	3.40 ± 0.05	0.640 ± 0.010	1.70 ± 0.06	
2-ketovalerate						not determined
k_{cat} (s^{-1})	13.7 ± 0.1	14.6 ± 0.1	4.81 ± 0.05	1.97 ± 0.03	4.64 ± 0.06	
K_m (mM)	12.9 ± 0.2	15.0 ± 0.3	14.8 ± 0.4	19.3 ± 0.7	17.5 ± 0.6	
k_{cat}/K_m (mM^{-1} s^{-1})	1.07 ± 0.01	0.98 ± 0.01	0.325 ± 0.007	0.101 ± 0.002	0.271 ± 0.005	
ThDP K_c (μM)	1.96 ± 0.07	1.55 ± 0.03	8.68 ± 0.19	21.7 ± 0.6	45.3 ± 1.3	>500
Mg^{2+} K_c (μM)	8.66 ± 0.58	10.3 ± 0.3	193 ± 5	410 ± 6	451 ± 13	>6000

gave very similar activities to the wild-type. Deletion of R561 caused a drop to about 40% of wild-type and further deletion of S560 reduced the activity to just a few percent of wild-type. Deletion of the next five residues also yielded enzymes with a small fraction of wild-type but deletion of R554 and beyond gave no detectable activity.

E. coli cell extracts contain lactate dehydrogenase activity that can be mistaken for PDC. Corrections for this activity cause no great inaccuracy for the high PDC activity observed with wild-type but are not reliable when PDC activity is low. Consequently, five of the deletion mutants were chosen for purification and further characterization. These were the enzymes with seven residues deleted (designated Δ7), Δ8, Δ9, Δ11, and Δ15. This series covers the range from the largest deletion yielding an enzyme with apparently normal activity (Δ7) through to the smallest deletion that appeared to abolish activity (Δ15). Enzymes with deletions larger than Δ15 tended to aggregate and proved to be too unstable to purify. Each of the proteins that was purified appeared to be close to purity, as indicated by SDS−PAGE (data not shown). In gel filtration chromatography, wild-type PDC eluted just before β-amylase (200 kDa) suggesting that the enzyme is a homotetramer of its 60.8 kDa subunits. The deletion mutants tested (Δ7, Δ8, Δ9, and Δ11) also eluted at a similar position and it is concluded that these deletions do not alter the quaternary structure of the enzyme.

Kinetic Properties of Δ7, Δ8, Δ9, Δ11, and Δ15. The kinetic properties of these enzymes are summarized in Table 2. The specific activities and k_{cat} values broadly confirmed the observations made with cell extracts. Deletion of seven residues does not decrease the specific activity; indeed, a small increase was observed. Removal of R561 (Δ8) caused the specific activity to drop substantially and deletion of S560 (Δ9) resulted in a specific activity that is about 5% of wild-type. Δ11 has slightly lower specific activity than Δ9 and Δ15 has a very low, but clearly nonzero, activity.

The K_m value for pyruvate shows only small variations across the series of mutants and ranged from 0.5 (Δ15) to 1.39 (Δ8) mM. The data show a discernible trend with Δ7 and Δ8 having a K_m that is approximately double the wild-type value followed by a gradual decrease through Δ9, Δ11, and Δ15 to a value that is 74% of wild-type. Although these changes are relatively small, they were quite reproducible. The k_{cat}/K_m values of the truncation mutants are all lower than that of wild-type with Δ7 and Δ8 showing values that are 61 and 12% of wild-type, respectively. Δ9 and Δ11 are each about 4% of wild-type while Δ15 is a mere 0.2%. For the most part, the effects on k_{cat} dominate the changes in k_{cat}/K_m because the K_m values of the mutants are fairly similar to that of wild-type.

We have shown previously (*26*) that wild-type *Z. mobilis* PDC is capable of catalyzing the decarboxylation of both 2-ketobutyrate and 2-ketovalerate, albeit with lower efficiency than its activity with pyruvate. The ability of the various truncation mutants (except Δ15) to use these alternative substrates was therefore tested. The K_m value for 2-ketobutyrate tends to increase through the deletion series while k_{cat} rises above the wild-type value (Δ7) and then falls below (Δ8, Δ9, and Δ11). Although the k_{cat}/K_m for 2-ketobutyrate is in all cases lower than that for pyruvate, it is of interest that Δ8 has the same k_{cat} for 2-ketobutyrate as it has for pyruvate, while Δ9 and Δ11 each has a higher k_{cat} for 2-ketobutyrate than it has for pyruvate by factors of 1.9 and 6.8, respectively. Trends were less obvious for 2-ketovalerate although the k_{cat}/K_m for this substrate, compared to that for pyruvate, is higher for all mutants than it is for wild-type. For example, wild-type shows a preference for pyruvate over 2-ketovalerate (as judged by the ratios of k_{cat}/K_m) by a factor of 155, while the corresponding values for Δ7, Δ8, Δ9, and Δ11 are 103, 63, 64, and 27.

Removal of the cofactors, ThDP and Mg^{2+}, abolishes activity and this can be fully restored by addition of the cofactors. The dependence of activity on the concentration of each cofactor added can be used to calculate a cofactor activation constant (K_c) that is an approximate measure of the affinity of the enzyme for ThDP and Mg^{2+} (Table 2). Very clear trends are obvious in the data; Δ7 is similar to wild-type but Δ8, Δ9, Δ11 and Δ15 show progressive increases in the K_c values. For the last member of this series, the values were too high to measure accurately but are certainly several hundred-fold higher than those of wild-type.

Substitution Mutations at R561 and S560. The results described above established that the last seven residues of PDC are unimportant and that the next few are critical for activity, cofactor binding and substrate specificity. We therefore went on to prepare specific mutants at positions 560 and 561 to determine the influence of the particular residues. As with the deletion series described earlier, we first assayed for PDC activity in cell extracts (Table 3). In the nomenclature that we have adopted for these mutated enzymes, Δ8+X represents deletion of eight residues but with amino acid X added at the carboxyl-terminus. In this

Table 3: Activity of S560 and R561 Substitution Mutants of PDC[a]

enzyme activity	specific (% wild-type)
Δ8+R (=Δ7)	100
Δ8+C	49−65
Δ8+E	48−49
Δ8+L	36−41
Δ8+P	20−30
Δ8+S	66−81
Δ8+T	63−69
Δ8+Y	58−76
Δ9+S (=Δ8)	38−42
Δ9+L	36−39
Δ9	1−2

[a] For each mutant, cell extracts of several clones were assayed; the range of measured specific activities are reported.

nomenclature, Δ8+R is the same as Δ7 because the last residue (561) of Δ7 is arginine. Each of these mutated enzymes appeared to be similar to one another, with activities (compared to wild-type) ranging from 20 to 30% (Δ8+P) to 66−81% (Δ8+S); these activities span the value observed for Δ8 (38−42%). Four of these mutants (Δ8+E, Δ8+L and Δ8+P, and Δ9+L) were selected for further study; in each case, these represent a radical substitution in the wild-type sequence (R to E, L or P at position 561, and S to L at position 560).

Each of the proteins was purified and judged to be close to purity, as indicated by SDS−PAGE (data not shown). Each of them eluted very close to wild-type in gel filtration chromatography, suggesting that each is homotetrameric. Their kinetic properties were determined and these are shown in Table 4; to assist in comparison with Δ7, Δ8, and Δ9, data from these mutants that were shown in Table 2 are reproduced in Table 4. No two of these substitution mutants are identical in all respects but, for the most part, they are quite similar to Δ8 and clearly different from both Δ7 and Δ9. Thus, any substitution of R561 is approximately equivalent to deleting R561 entirely, showing that the side-chain of this residue plays an important role. In contrast, the substitution at S560 made little difference, consistent with the proposition that it is backbone atoms rather than the side chain of this serine that control the difference between Δ8 and Δ9.

Rate Constants for Cofactor Binding and Release. The cofactor activation constants reported in Tables 2 and 4 are combined constants that depend on the rate constants for binding (k_{on}) and release (k_{off}), as well as those of other steps in the catalytic cycle. Cofactor binding in the absence of substrate is accompanied by quenching of the fluorescence of W487 (*21*, *27*) due to a change in the local environment at the subunit interface (*28*). Measurements of the time course of fluorescence quenching (Figure 3A) allow an apparent first-order rate constant to be determined by fitting eq 2 to the data. A series of such analyses, at various cofactor concentrations, allow k_{on} and k_{off} to be determined from the resulting linear relationship (eq 3; Figure 3B). Two of the

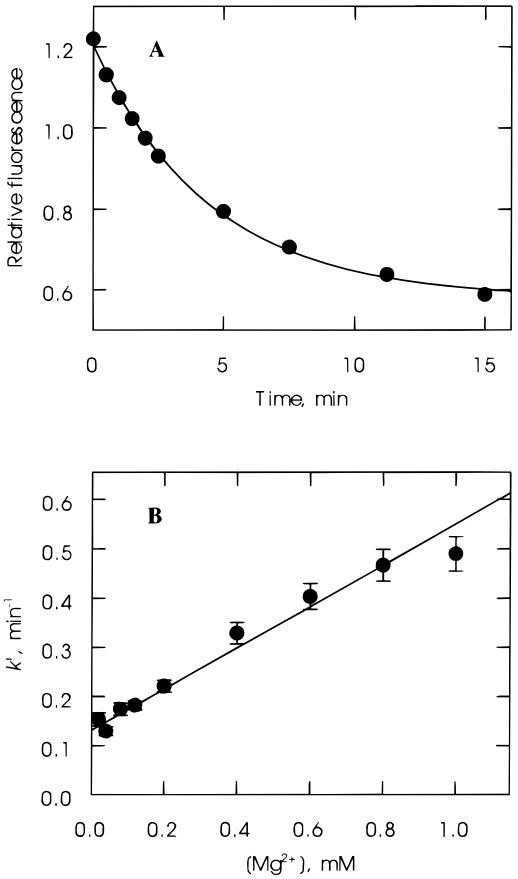

FIGURE 3: Cofactor binding by *Z. mobilis* PDC. Panel A shows tryptophan fluorescence as a function of time for the D8+L PDC mutant at ThDP and Mg^{2+} concentrations of 0.1 and 0.2 mM, respectively. The line represents the fitted curve using eq 2. The apparent first-order rate constant obtained at this, and a series of other, Mg^{2+} concentrations are plotted in panel B; from the slope and intercept, respectively, of the fitted straight line (eq 3) the values of k_{on} and k_{off} are obtained.

Table 4: Kinetic Properties of PDC Mutants with Substitutions at S560 and R561

enzyme	Δ7 (=Δ8+R)	Δ8+E	Δ8+L	Δ8+P	Δ8 (=Δ9+S)	Δ9+L	Δ9
specific activity (units/mg)	103	33.1	27.3	17.2	24.3	21.9	4.5
pyruvate							
k_{cat} (s^{-1})	135 ± 1	41.7 ± 0.3	32.5 ± 0.2	22.9 ± 0.1	28.6 ± 0.1	27.0 ± 0.1	5.29 ± 0.02
K_m (mM)	1.35 ± 0.02	1.26 ± 0.02	1.14 ± 0.02	1.03 ± 0.02	1.39 ± 0.02	0.99 ± 0.01	0.82 ± 0.01
k_{cat}/K_m (mM^{-1} s^{-1})	101 ± 1	33.0 ± 0.5	28.6 ± 0.4	22.3 ± 0.4	20.5 ± 0.2	27.2 ± 0.3	6.43 ± 0.08
2-ketobutyrate							
k_{cat} (s^{-1})	82.2 ± 0.4	39.9 ± 0.5	53.5 ± 0.5	42.5 ± 0.5	30.1 ± 0.2	55.6 ± 0.7	10.3 ± 0.11
K_m (mM)	4.44 ± 0.07	6.60 ± 0.22	9.19 ± 0.23	10.3 ± 0.3	8.86 ± 0.18	11.7 ± 0.4	16.1 ± 0.4
k_{cat}/K_m (mM^{-1} s^{-1})	18.5 ± 0.2	6.05 ± 0.15	5.82 ± 0.10	4.14 ± 0.10	3.40 ± 0.05	4.75 ± 0.10	0.640 ± 0.010
2-ketovalerate							
k_{cat} (s^{-1})	14.6 ± 0.1	6.34 ± 0.08	9.60 ± 0.08	7.04 ± 0.12	4.81 ± 0.05	7.42 ± 0.04	1.97 ± 0.03
K_m (mM)	15.0 ± 0.3	15.5 ± 0.6	15.1 ± 0.4	15.7 ± 0.8	14.8 ± 0.4	16.9 ± 0.2	19.3 ± 0.7
k_{cat}/K_m (mM^{-1} s^{-1})	0.980 ± 0.010	0.410 ± 0.010	0.640 ± 0.010	0.450 ± 0.020	0.325 ± 0.007	0.440 ± 0.005	0.101 ± 0.002
ThDP K_c (μM)	1.55 ± 0.03	7.42 ± 0.15	4.13 ± 0.07	6.51 ± 0.12	8.68 ± 0.19	5.76 ± 0.06	21.7 ± 0.6
Mg^{2+} K_c (μM)	10.3 ± 0.3	308 ± 11	53.6 ± 1.2	142 ± 4	193 ± 5	55.6 ± 1.0	410 ± 6

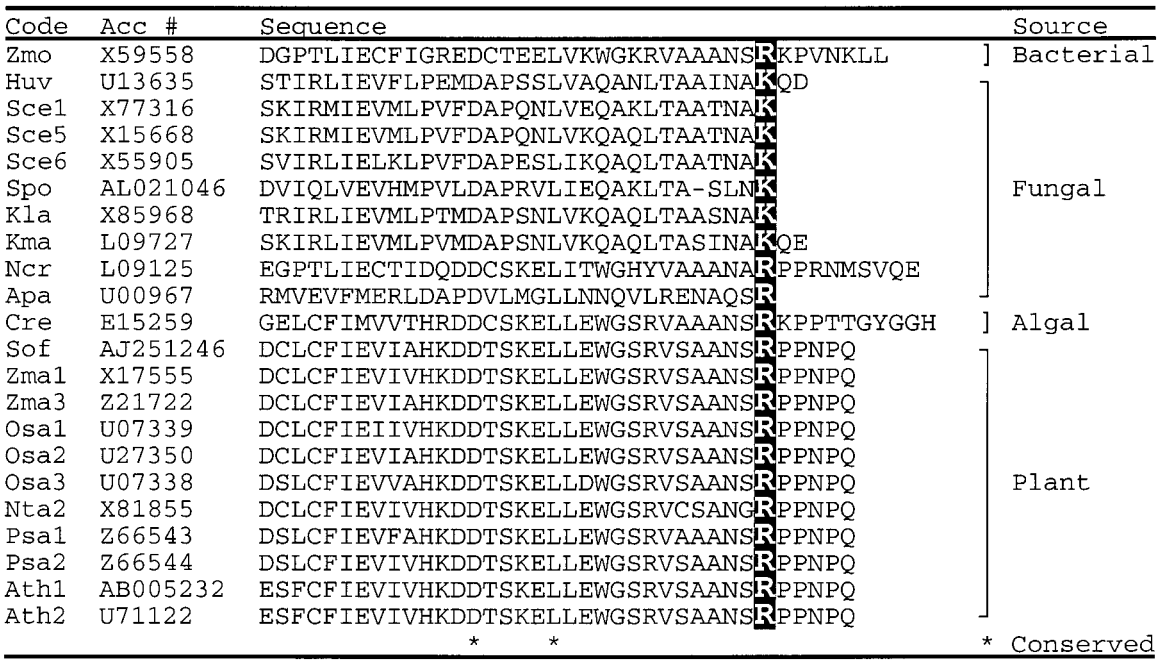

FIGURE 4: Alignment of the carboxyl-terminal region of various PDC protein sequences. The species abbreviations are Apa, *Aspergillus parasiticus*; Ath, *Arabidopsis thaliana*; Cre, *Chlamydomonas reinhardii*; Huv, *Hanseniaspora uvarum*; Kla, *Kluyveromyces lactis*; Kma, *K. marxianus*; Ncr, *Neurospora crassa*; Nta, *Nicotiana tabacum*; Osa, *Oryza sativa*; Psa, *Pisum sativum*; Sce, *Saccharomyces cerevisiae*; Sof, *Saccharum officinarum*; Spo, *Schizosaccharomyces pombe*; Zma, *Zea mays*; Zmo, *Z. mobilis*. Arabic numerals following species abbreviation indicate the products of different genes. Totally conserved residues are shown by an asterisk (*), while the residue equivalent to R561 of *Z. mobilis* PDC is highlighted.

Table 5: Rate Constants for Cofactor Binding and Release by Wild-Type and by Mutants of PDC

	ThDP		Mg^{2+}	
enzyme	k_{on} (mM^{-1} h^{-1})	k_{off} (h^{-1})	k_{on} (mM^{-1} h^{-1})	k_{off} (h^{-1})
wild-type	1110 ± 30	3.53 ± 0.75	132 ± 3	2.39 ± 0.53
Δ8+L	297 ± 17	10.26 ± 0.67	26 ± 1	7.91 ± 0.56
Δ9	110 ± 10	4.57 ± 1.62	0.85 ± 0.08	8.34 ± 0.47

altered enzymes were chosen for such an analysis, representing a moderate (Δ8+L) and large (Δ9) decrease in affinity for cofactors, and compared with the wild-type enzyme (Table 5).

The rate constants for release of each cofactor (k_{off}) showed relatively small variations from wild-type. However, the values of k_{on} changed substantially and showed clear trends which indicate that the dominant factor in decreased cofactor affinity in the mutants is a reduction in the rate of binding.

DISCUSSION

PDC genes and/or cDNAs have been isolated and sequenced from a number of organisms and an alignment of the carboxyl-terminal region is shown in Figure 4. There is little overall conservation of sequence with only two residues (D543 and L548) identical in all PDCs although sub-groups, such as the plant sequences, are very similar to one another. However, it is noteworthy that every sequence extends to or beyond a position equivalent to R561 of *Z. mobilis* PDC, and the residue at this position is invariably arginine or lysine. These observations are fully consistent with our data in which residues beyond R561 are unnecessary for PDC function, and deletion or radical substitution of this residue affects significantly the properties of the enzyme. Although we have not made the Δ8+K mutant of *Z. mobilis* PDC, we anticipate that it would be more similar to Δ7 than to Δ8.

The carboxyl-terminal region of PDC appears to play three roles. First, it allows proper closure of the active site and deletion results in drastic decreases in k_{cat} with little effect on K_m. This means that the effect on k_{cat}/K_m parallels that on k_{cat} itself, an observation that can be interpreted in two ways. One possibility is that several rate constants are affected and that there are compensatory changes which result in a reduction in k_{cat} while not affecting K_m. The simpler interpretation is that only the one rate constant common to k_{cat} and k_{cat}/K_m is affected; that is, decarboxylation of the lactyl-ThDP intermediate is the step that is impaired. We have described previously (*16*, *20*) a quantitative kinetic model of wild type *Z. mobilis* PDC (Figure 5) that agrees extremely well with the kinetic data reported in Table 2 and that would accommodate these results. The conclusion that active site closure is required for decarboxylation is entirely consistent with earlier studies (*12*, *13*) in which it was deduced that the active site must be protected from solvent in order for this reaction to occur.

The second role of the carboxyl terminus is manifested in the affinity of the enzyme for its cofactors. As more of this region is deleted there is a progressive decrease in the ability of the enzyme to bind both Mg^{2+} and ThDP. We had anticipated that there would be a higher rate of release when the carboxyl terminus is deleted due to a failure to close, and thereby retain the cofactors. This turned out not to be the case; there is little change in the rate constant for release but major effects on the rate constant for cofactor binding. Possibly this reflects a slowing of the locking down of the carboxyl terminus rather than an effect on the initial enzyme-cofactor encounter complex. In this context, we note that a conformational change upon cofactor binding by PDC has

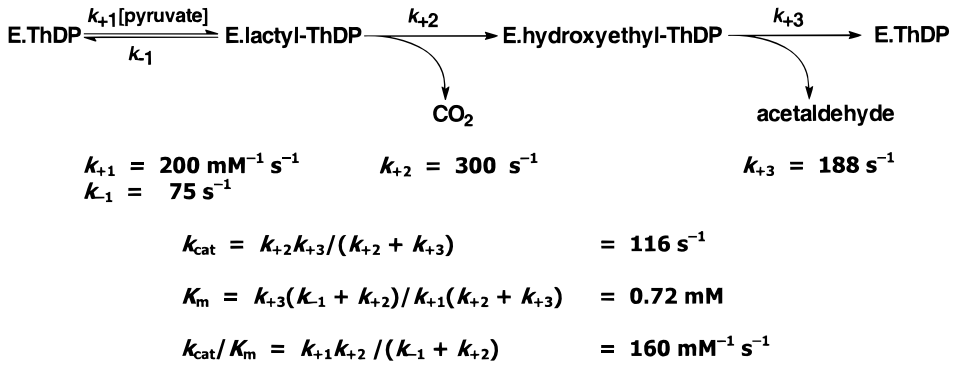

FIGURE 5: Quantitative kinetic model of the catalytic cycle of wild-type *Z. mobilis* PDC. This model was first suggested by Sun et al. (*16*) and later modified by Chang et al. (*20*). The calculated values of k_{cat} (116 s^{-1}), K_m (0.72 mM), and k_{cat}/K_m (160 mM^{-1} s^{-1}) are in close agreement with the experimental values (Table 2) of 113 s^{-1}, 0.68 mM and 166 mM^{-1} s^{-1}.

been proposed by several groups based on solution X-ray scattering studies (*29*) and the kinetics of holoenzyme reconstitution (*21*, *30*, *31*). Although the nature of this conformational change has not been elucidated, we suggest that closure of the active site by the carboxyl-terminal region could represent an important component of the change.

The third effect of deletion of the carboxyl terminus is a broadening of substrate specificity so that the enzyme shows an improvement it its ability to decarboxylate 2-ketobutyrate and 2-ketovalerate, relative to the activity with pyruvate. As with pyruvate, the effects of truncation on the kinetics toward these larger substrates are reflected primarily in the values of k_{cat} (and k_{cat}/K_m), rather than in those of K_m itself. We suggest that in the wild-type enzyme there is tight closure of the active site that severely limits the ability of the enzyme to accommodate substrates larger than pyruvate. Truncation of the carboxyl terminus results in more flexibility and imposes fewer constraints on the size of the substrate. However, no deletion had a large effect on the K_m value for any one substrate, which indicates that there are no specific interactions between the substrate and any of the deleted residues. The possibility of specific interactions with residues more remote from the carboxyl terminus than K553 could not be tested due to instability of the proteins.

It is of interest that the largest deletion, of 15 residues, reduces k_{cat} by a factor of 600-fold only. This is rather a small change and implies that active site closure assists in, but is not essential for, catalysis. In general, PDC seems to be rather tolerant of changes around the catalytic center and, of the active site mutants whose properties have been properly characterized (*1*, *20*, *22*), only the H113Q mutant appears to be completely inactive. Even after mutation of the "catalytic glutamate" (*28*) the enzyme retains up to 3% of its activity. This seems to be a general feature of ThDP-dependent enzymes and mutations of the equivalent glutamate residue in transketolase (*32*) and the pyruvate dehydrogenase E1 component (*33*) also result in significant residual activity. Possibly this is because one of the main functions of the active site of these enzymes is to promote the ionization of the C2 proton of ThDP (*8*, *34*). No single residue is indispensable in this process and most mutations result in an active, albeit crippled, enzyme.

The weight of evidence from the present study point toward a model in which the carboxyl-terminal region of PDC moves aside to allow substrate access, closes during catalysis, then opens again to release the reaction products. However, we should stress that there is no direct evidence for this movement. Although the crystal structure of *Z. mobilis* PDC (*5*) clearly shows that access to the active site is impeded by the carboxyl terminus, it is possible that the structure of the enzyme in solution is slightly different from that in crystals. We are now attempting to obtain more direct evidence for movement of this region of PDC during catalysis.

REFERENCES

1. Candy, J. M., and Duggleby, R. G. (1998) *Biochim. Biophys. Acta 1385*, 323−338.
2. Dyda, F., Furey, W., Swaminathan, S., Sax, M., Farrenkopf, B., and Jordan, F. (1993) *Biochemistry 32*, 6165−6170.
3. Arjunan, P., Umland, T., Dyda, F., Swaminathan, S., Furey, W., Sax, M., Farrenkopf, B., Gao, Y., Zhang, D., and Jordan, F. (1996) *J. Mol. Biol. 256*, 590−600.
4. Lu, G., Dobritzch, D., König, S., and Schneider, G. (1997) *FEBS Lett. 403*, 249−253.
5. Dobritzsch, D., König, S., Schneider, G., and Lu, G. (1998) *J. Biol. Chem. 273*, 20196−20204.
6. Chabrière, E., Charon, M. H., Volbeda, A., Pieulle, L., Hatchikian, E. C., and Fontecilla-Camps, J.-C. (1999) *Nat. Struct. Biol. 6*, 182−190.
7. Hawkins, C. F., Borges, A., and Perham, R. N. (1989) *FEBS Lett. 255*, 77−82.
8. Kern, D., Kern, G., Neef, H., Tittmann, K., Killenberg-Jabs, M., Wikner, C., Schneider, G., and Hübner, G. (1997) *Science 275*, 67−70.
9. Ermer, J., Schellenberger, A., and Hübner, G. (1992) *FEBS Lett. 299*, 163−165.
10. Harris, T. K., and Washabaugh, M. W. (1995) *Biochemistry 34*, 14001−14011
11. Lobell, M., and Crout, D. H. G. (1996) *J. Chem. Soc., Perkin Trans. 1*, 1577−1581.
12. Crosby, J., Stone, R., and Lienhard, G. E. (1970) *J. Am. Chem. Soc. 92*, 2891−2900.
13. Kluger, R., and Smyth, T. (1981) *J. Am. Chem. Soc. 103*, 1214−1218.
14. Lobell, M., and Crout, D. H. G. (1996) *J. Am. Chem. Soc. 118*, 1867−1873.
15. Alvarez, F. J., Ermer, J., Hübner, G., Schellenberger, A., and Schowen, R. L. (1995) *J. Am. Chem. Soc. 117*, 1678−1683.
16. Sun, S. X., Duggleby, R. G., and Schowen, R. L. (1995) *J. Am. Chem. Soc. 117*, 7317−7322.
17. Kluger, R., Lam, J. F., and Kim, C.-S. (1993) *Bioorg. Chem. 21*, 275−283.
18. Sambrook, J., Fritsch, E. F., and Maniatis, T. (1989) *Molecular cloning: a laboratory manual*, 2nd ed., Cold Spring Harbor Laboratory Press, Plainview, NY.
19. Candy, J. M., and Duggleby, R. G. (1994) *Biochem. J. 300*, 7−13.

20. Chang, A. K., Nixon P. F., and Duggleby, R. G. (1999) *Biochem. J. 339*, 255−260.
21. Diefenbach, R. J., and Duggleby, R. G. (1991) *Biochem. J. 276*, 439−445.
22. Schenk, G., Leeper, F. J., England, R., Nixon, P. F., and Duggleby, R. G. (1997) *Eur. J. Biochem. 248*, 63−71.
23. Laemmli, U. K. (1970) *Nature 227*, 680−685.
24. Sedmac, J. J., and Grossberg, S. E. (1977) *Anal. Biochem. 79*, 544−552.
25. Duggleby, R. G. (1984) *Comput. Biol. Med. 14*, 447−455.
26. Huang, C.-Y., Nixon P. F., and Duggleby, R. G. (1998) *J. Biochem. Mol. Biol. 32*, 39−44.
27. Diefenbach, R. J., Candy, J. M., Mattick, J. S., and Duggleby, R. G. (1992) *FEBS Lett. 296*, 95−98.
28. Candy, J. M., Koga, J., Nixon, P. F., and Duggleby, R. G. (1996) *Biochem. J. 315*, 745−751.
29. Hübner, G., König, S., Schellenberger, A., and Koch, M. H. J. (1990) *FEBS Lett. 266*, 17−20.
30. Schellenberger, A., and Hübner, G. (1967) *Hoppe-Seyler's Z. Physiol. Chem. 348*, 491−500.
31. Vaccaro, J. A., Crane, E. J., III, Harris, T. K., and Washabaugh, M. W. (1995) *Biochemistry 34*, 12636−12644.
32. Wikner, C., Meshalkina, L., Nilsson, U., Nikkola, M., Lindqvist, Y., Sundström, M., and Schneider, G. (1994) *J. Biol. Chem. 269*, 32144−32150.
33. Fang, R., Nixon, P. F., and Duggleby, R. G. (1998) *FEBS Lett. 437*, 273−277.
34. Harris, T. K., and Washabaugh, M. W. (1995) *Biochemistry 34*, 13994−14000.

BI0002683